coatings

MDPI

Article

Microstructure and Mechanical Properties of Electrically Assisted Brazing Joints of Dissimilar Aluminum and Steel Alloys

Kun Gao [1,2,*], Guiqi Liu [2], Xiaojun Sun [2] and Yu Wang [3]

[1] School of Mechanical Engineering, Anhui Polytechnic University, Wuhu 241000, China
[2] Automobile and Traffic Engineering, Liaoning University of Technology, Jinzhou 121001, China
[3] School of Mechanotronic Technology, Changzhou Vocational Institute of Textile and Garment, Changzhou 213000, China
* Correspondence: 18217603739@163.com

Abstract: The microstructure and mechanical properties of electrically assisted brazing (EA-brazing) joints of aluminum alloy 6061-t6 (AA6061-t6) and S45C steel are experimentally investigated. During the EA-brazing process, an electric current is directly applied to the cylindrical specimen assembly (S45C and AA6061-t6) and fillers of 88% Al and 12% Si (in the middle of the specimen assembly). The temperature of the specimen assembly rises rapidly to the melting point of the filler and remains nearly constant for a period of time using a pulsed electric current. Two types of EA-brazing joints are fabricated, namely Joint-0s (no temperature holding time) and Joint-12s (12 s temperature holding time). The characteristics of the intermetallic compounds (IMCs) formed at the EA-brazing joint interface are analyzed using scanning electron microscopy and energy dispersive spectrometer. Compared to Joint-0s, the Fe-rich IMCs (FeAl) are observed at the interface of Joint-12s due to the 12 s temperature holding time. In addition, the microstructural analysis shows that the thickness of the diffusion layer increases with increasing temperature holding time. The mechanical properties of the EA-brazing joints are evaluated using bending tests. The results of the mechanical test show that the strength of Joint-12s is higher than that of Joint-0s.

Keywords: electrically assisted brazing; aluminum alloys; steel; mechanical properties

Citation: Gao, K.; Liu, G.; Sun, X.; Wang, Y. Microstructure and Mechanical Properties of Electrically Assisted Brazing Joints of Dissimilar Aluminum and Steel Alloys. *Coatings* **2024**, *14*, 213. https://doi.org/10.3390/coatings14020213

Academic Editors: Francisco J. Flores-Ruiz and Saideep Muskeri

Received: 11 January 2024
Revised: 4 February 2024
Accepted: 6 February 2024
Published: 7 February 2024

1. Introduction

In recent years, lightweight composite structures have attracted significant attention since they can reduce environmental pollution and unnecessary energy waste. Steel and aluminum (Al) alloys are the most widely used alloys in the modern manufacturing industry. Even though steel has the advantages of low price, good weldability, and better mechanical properties, its poor corrosion resistance and heavy weight limit its application in lightweight structures. In contrast, Al alloys with the advantages of light weight and good corrosion resistance can overcome the weakness of steel. Therefore, the Al-steel composite structure, which possesses excellent advantages and performance, has wide applications in the automobile, aerospace, and railway industries [1,2]. Unfortunately, the joining of these two alloys imposes complications due to the vast differences in their physical and chemical properties.

To date, joining steel and Al alloys is still an enormous challenge. Previous works show two main joining methods of steel and Al alloys: conventional fusion welding and solid-state joining [3,4]. Some studies show that the conventional fusion welding of steel and Al alloys leads to the formation of large brittle intermetallic compounds (IMCs), which are detrimental to the mechanical properties of the joint [5–7]. In addition, fusion welding technologies can lead to the formation of residual stress inside the joints because they require extensive heat to melt the base metals, which significantly reduces the mechanical properties of the joint. In contrast, solid-state welding (without melting the base metals) has been employed for joining dissimilar metals of steel and Al alloys, such as explosive

welding, friction stir welding, and electrically assisted pressure joining. However, the shape and size of these solid-state joining joints are extremely restricted [8–10]. Explosion welding, which requires large plastic deformation to join workpieces, is generally limited to welding components with a high-ductility material [11]. A rotating tool is used to generate frictional heat to plasticize and stir the materials in the friction stir welding process [12]. To summarize, these solid-state welding techniques require large plastic deformations to join metals during the welding process. Unfortunately, it is necessary for welding very thin metal sheets to protect the workpiece from large plastic deformations during the welding process. These above solid-state welding technologies cannot overcome this shortcoming, which requires deformation.

As a solid-state welding technology, brazing is becoming popular for joining very thin metal sheets with dissimilar materials to avoid the formation of large amounts of IMCs in the fusion welding process and to reduce residual stress. Also, compared with other solid-state welding technologies, brazing processes possess several advantages, such as rapid and local heating, minimal formation of IMCs, and non-essential large plastic deformation of the workpiece due to lower heat input [13]. Liu et al. [14] reported that a joint of 1060 Al and stainless steel using Al–Si–Cu filler metal was fabricated successfully using the brazing process. Yang et al. [15] found that the different content of Zirconium (Zr) in Al-based filler has an important influence on the brazing joint of 6061 Al alloy to 304 stainless steel. Dong et al. [16] researched the effect of the IMC layer at the joint interface on the strength of steel/Al TIG welding-brazing using different types of filler metal in lap joints. However, current brazing technologies, such as MIG arc brazing [17] and laser brazing [18], require expensive and complex equipment to join workpieces with simple shapes.

Electrically assisted brazing (EA-brazing) is one kind of brazing (solid-state welding) process which employs heat resistance to join metals. In EA-brazing, direct current is employed to melt the filler. EA-brazing possesses several technical advantages over conventional brazing, such as cost-effective process facilities, much shorter process times (a few seconds), and electrodes with different shapes to join complex-shaped workpieces. In the EA-brazing process, an electric current is directly applied to melt the filler and join the specimens under a small amount of static load used to fix the specimens and filler. Previous research indicated that direct current in the EA-brazing process can promote the diffusion of metal elements due to the directional flow of electrons [19]. In addition, the energy loss to the environment is less in EA-brazing compared with induction heating. The EA-brazing of steel and Al alloys employs fillers to diffuse elements between both dissimilar metals during welding. Therefore, for the brazing of steel and Al alloys, filler plays an important role in the joining process [20].

In the present investigation, we explored the unique features of EA-brazing of S45C and AA6061-t6 using Al-based filler metals. The microstructure of the EA-brazing joints was observed by using optical microscopy and a field emission scanning electron microscope. Also, the elemental diffusion at the joint interface between the filler and specimens (S45C and AA6061-t6) was studied. Finally, the mechanical properties of the EA-brazing joints were analyzed.

2. Experimental Process

The specimens employed in the present study are cylindrical bulk metals of S45C and AA6061-t6 with a diameter of 15 mm and a height of 10 mm (Figure 1). The chemical compositions of the base materials (S45C and AA6061-t6) and the filler metal (Al718) are listed in Table 1. Prior to the EA-brazing experiments, the joining surfaces of the specimens were carefully polished using 320-grit and 600-grit sandpapers to remove the rust (on S45C steel) and oxide layers (on AA6061-t6). Finally, the specimens were thoroughly cleaned with acetone to remove any grease or dirt.

To prepare EA-brazing, the Al-based filler (0.1 mm thick) was cut into approximately circular shapes with an identical diameter as the EA-brazing specimens. A custom-made fixture was installed in a servo press machine, as schematically shown in Figure 2. Resis-

tance heating was generated by direct current, which was produced using a programmable welder (VADAL SP-1000U, Hyosung, Seoul, Republic of Korea). A pair of electrodes was made of tool steel. To form a closed-loop circuit (the electrode, specimens, and direct current supply device), Bakelite insulators were placed between the electrode and the servo press machine.

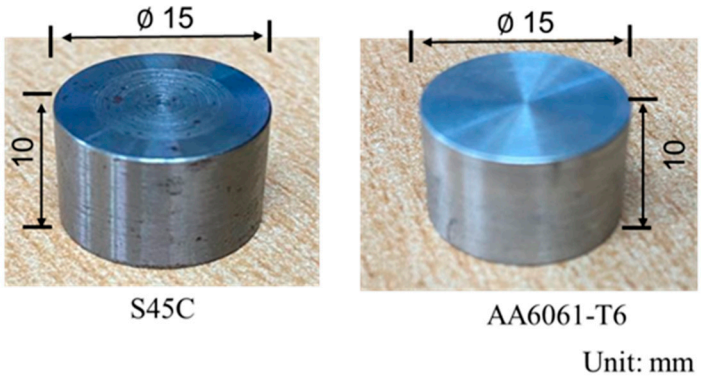

Figure 1. Cylindrical specimens of S45C and AA6061-t6 for EA-brazing joining.

Table 1. The nominal chemical compositions of the base materials (alloying elements, wt%).

	Fe	Al	Ni	Mn	Cu	Si	P	C	S	Zn	Ti
S45C	Bal.	--	0.2	0.6	0.25	0.15	0.03	0.42	0.035	--	--
AA6061-T6	0.7	Bal.	--	0.15	0.15	0.4	--	--	--	0.25	0.25
Al718 filler	--	Bal.	--	--	--	12	--	--	--	--	--

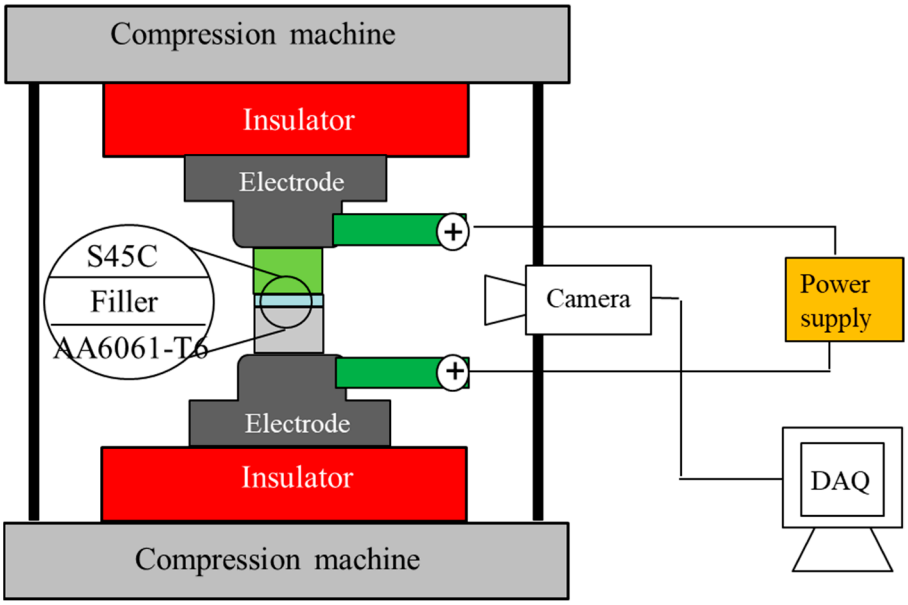

Figure 2. Schematic of EA-brazing experimental setup.

During EA-brazing, the filler was placed at the interface between the two brazing specimens. A preload of 1000 N was applied to fix the specimen assembly to ensure good contact between the brazing specimens and electrodes. A direct current was applied to the specimen assembly and filler during the EA-brazing process, as shown in Figure 3.

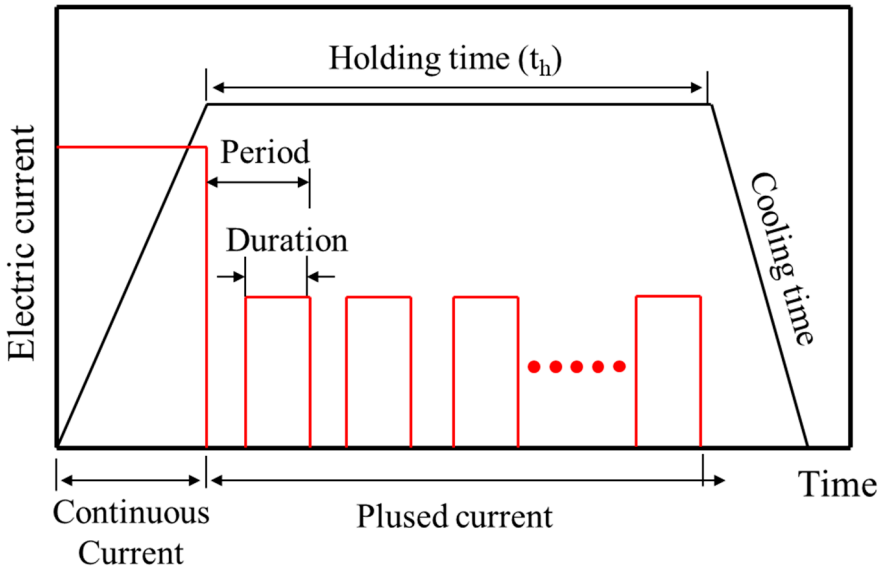

Figure 3. Schematic of applying electric current in the EA-brazing process.

The electric current parameter combination (Table 2) is divided into two parts: a continuous electric current and a pulsed electric current. In the beginning, a continuous electric current was applied to raise the temperature to the melting point of the filler. Afterwards, several cycles of pulsed electric current were applied to the specimen assembly to maintain the temperature and promote elemental diffusion between the filler and specimens. In this study, two electric current parameter combinations were considered: only continuous electric current (no holding time) and continuous electric current plus nine cycles of pulsed electric current (holding time of 12 s). Since the compositions and physical properties of AA6061-t6 are similar to those of the filler, the temperature of the AA6061-t6 during joining was continuously monitored and recorded using an infrared thermal imaging camera (FLIR-T621, FLIR, Antennvägen, Sweden).

Table 2. Electric current parameters of joining experiments.

Step	Current Duration (s)	Current Intensity (kA)	Pulse Period (s)	Total Time (s)
Continuous current	5	3.8	0	5
Pulsed current	1.1	1.65	1.5	12

After the brazing experiment, the cross-sectional specimens were cut along the height direction at the center of the EA-brazing joints for microstructural observation. Firstly, optical microscopy (OM) (DM2700 M, Leica Corp., Wetzlar, Germany) was employed to observe whether there were defects in the joining interface of the EA-brazing joints. To further study the joining interfaces of the EA-brazing joints, their microstructures were examined using a field emission scanning electron microscope (FE-SEM: SU70, Hitachi, Hitachi-shi, Japan); moreover, the elemental contents at the joint interface were analyzed using an energy dispersive spectrometer (EDS: X-Max50, Horiba, Kyoto, Japan).

To further analyze the mechanical properties of the EA-brazing joints of S45C and AA6061-t6, the hardness properties of the EA-brazing joint of S45C and AA6061-t6 was evaluated using a Vickers indenter (HM-100, Mitutoyo, Kawaguchi, Japan) with a load of 2.94 N and a dwell time of 10 s. In addition, the EA-brazing joints were fixed on a homemade fixture (Figure 4), and their bending tests were performed using a universal

testing machine (Jianzhuo Instrument Technology Co., Ltd., Suzhou, China). Cross-sections of the shear-tested EA-brazing joint were observed by SEM and analyzed by EDS.

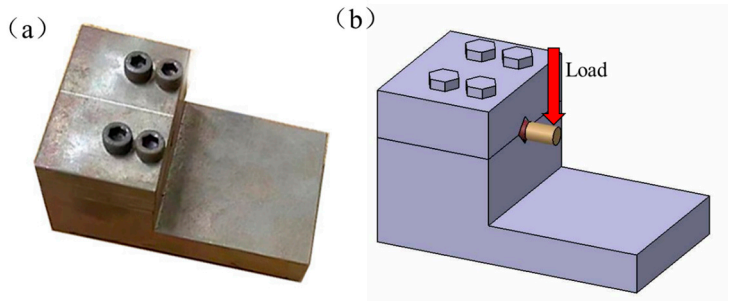

Figure 4. (**a**) Designed fixture for bending test; (**b**) schematic of the bending test of EA-brazing joints.

3. Results and Discussion

The AA6061-t6 temperature histories of Joint-0s and Joint-12s during EA-brazing were recorded, as shown in Figure 5. The temperature recorded at both EA-brazing joints increased from room temperature to 575 °C, which was lower than the melting point of AA6061-t6. The difference between both EA-brazing joints is that the temperature of Joint-12s was maintained between 550 °C and 575 °C for 12 s during the whole EA-brazing process time. Figure 6 shows that both EA-brazing joints with different temperature holding times were almost identical in appearance. Moreover, it can be seen that part of the filler was squeezed out between the steel and Al alloys during EA-brazing due to the thermal expansion of the specimens, which is why the temperature of Joint-12s cannot be kept constant.

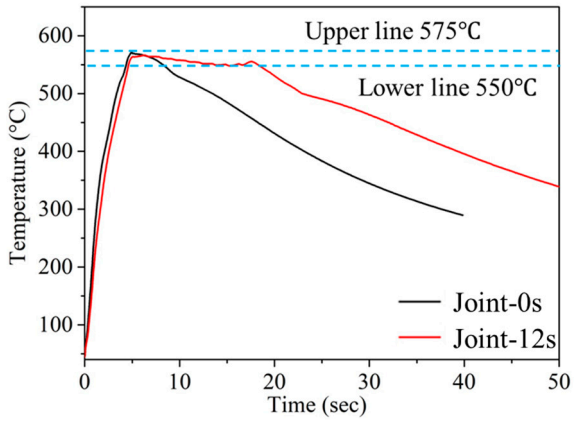

Figure 5. Maximum temperature histories during the EA-brazing process.

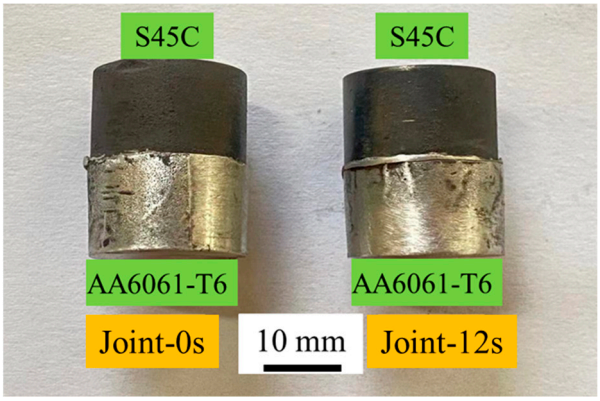

Figure 6. EA-brazing joints of S45C and AA6061-t6.

The cross-sections of both Al-steel dissimilar joints fabricated by the EA-brazing process are shown in Figure 7a,b. A clear interface between the steel and Al alloys was found in both EA-brazing joints. In addition, a few defects of various sizes (average size: 82.5 ± 9.3 μm) were observed at the Al/steel interfaces and characterized with an approximate ellipse, as marked by white rectanglein in Figure 7. One reason for the formation of voids on the surface of Al alloys is the poor contact between the specimens and the filler, which resulted in an excessive local temperature. Since the melting point of Al alloys is significantly lower than that of steel, the generation of high temperatures can cause the local melting of AA6061-t6 at the joining surface. The shrinkage of the melted filler during re-solidification is another cause of the defects at the joint interface [21]. Even so, the microscope defects were not observed in most interface areas of either joint.

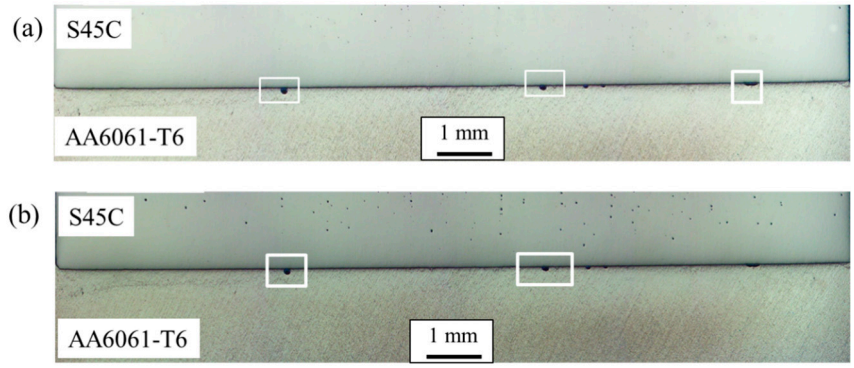

Figure 7. Cross-sections of EA-brazing joints: (**a**) Joint-0s (without holding time); (**b**) Joint-12s (with holding time of 12 s).

To further evaluate the joining area where no defects were observed by OM, the SEM images (Figures 8a and 9a) of the cross-section of both EA-brazing joints were analyzed. These results revealed that no microscopic defects were observed at the interface of either joint. Also, a distinct interlayer with different colors between the S45C steel (bright region) and AA6061-t6 (dark region) was observed at the interfaces of both the EA-brazing joints. The interlayer on the steel side at the interface of both joints between Al and steel (Figures 8a and 9a) had a relatively smooth boundary. In contrast, the interlayer on the Al alloy slide at the Al/steel interfaces of Joint-0s and Joint-12s observed from the two SEM images present an evident difference in shape. The interlayer of Joint-12s (Figure 9a) at the Al alloy side formed a more significant needle-like shape compared with that of Joint-0s. This could be explained by the fact that elements of Joint-12s at the interface of the filler and AA6061-t6 were promoted to diffuse due to more heat input caused by the 12 s holding time [22].

The elemental compositions of the layers of both the EA-brazing joints (Figures 8a and 9a) were identified by EDS point scans, as listed in Table 3. Based on the analysis of elemental compositions, the layers at the Al/steel interface of Joint-0s and Joint-12s can be confirmed as an Al/Fe IMC layer [23]. The results of the element analysis indicated that the Si of the IMC layers in both EA-brazing joints at representative locations (P1, P2, and P3) had lower concentrations than the filler layer, which suggested that the filler layer disappeared after the EA-brazing experiment. As mentioned in the experimental process, the filler with 0.1 mm thick used in the EA-brazing experiment was very thin. Most of the filler was squeezed out during the experiment process. Therefore, the reason for the disappearance of the filler can be explained as the element diffusion between the less remaining filler and base materials during the EA-brazing of steel and Al alloys. Combined with the Al-Fe phase diagram [24,25], the possible phases of the IMC layer of Joint-0s and Joint-12s can be deduced, as listed in Table 3. The possible phases of Joint-0s are mainly brittle Al-rich IMCs (Fe_2Al_5, $FeAl_2$, and $FeAl_3$). However, the possible phases of Joint-12s are composed of Fe-rich IMCs (FeAl) and Al-rich IMCs (Fe_2Al_5, $FeAl_2$ and $FeAl_3$). With increasing the temperature holding time, more quantities of Fe elements diffuse into the filler layer

and form the Fe-rich IMCs. Previous studies have indicated that Fe-rich IMCs cannot cause damage to the mechanical properties of the joints of steel and Al alloys [26,27]. The EDS line scans of both the EA-brazing joints with different temperature holding times are shown in Figures 8b and 9b. The concentrations of three different elements (Fe, Al, and Si) gradually change within three different zones (S45C, AA6061-t6, and IMC layer) for both the EA-brazing joints. Based on the changes in the element concentration, the thickness of the IMC layer at the interface of both ES-brazing joints can be approximately evaluated. The thickness of the IMC layer of Joint-12s with a temperature holding time (approximately 9.3 μm) is much larger than that of Joint-0s without a temperature holding time (approximately 6.8 μm). This result indicates that increasing the temperature holding time can significantly enhance the elemental diffusion at the faying surface of the base materials and filler [28].

Table 3. EDS analysis results of the IMC layers (at.%).

Joining Condition	Location	Compositions (at.%)			Possible Phase
		Al	Fe	Si	
Joint-0s	P1	76.65	21.61	1.74	$FeAl_3$, $FeAl_2$
	P2	73.72	24.04	2.24	$FeAl_3$, $FeAl_2$
	P3	62.13	36.69	1.18	Fe_2Al_5
Joint-12s	P1	72.66	26.21	1.13	$FeAl_3$, $FeAl_2$
	P2	58.72	40.04	1.24	Fe_2Al_5
	P3	50.25	47.96	1.79	FeAl

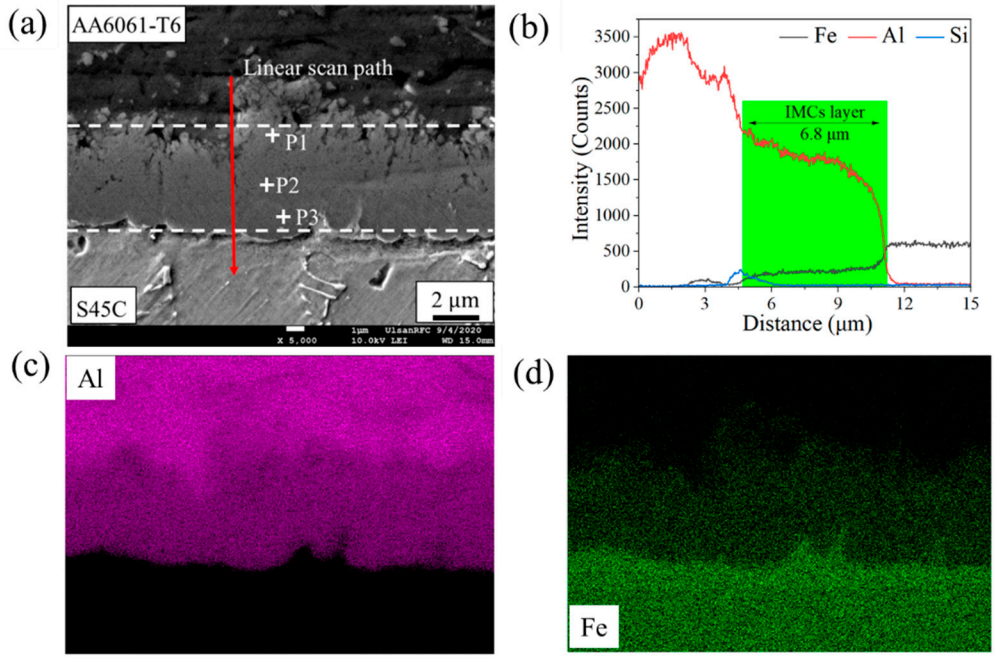

Figure 8. (**a**) SEM micrograph of Joint-0s, (**b**) elemental line scan across the joint interface, (**c**) Al distribution, and (**d**) Fe distribution.

The mechanical properties of the EA-brazing joints were evaluated using the hardness and bending tests. The microhardness profiles of both EA-brazing joints (Figure 10a) were approximately identical. For both EA-brazing joints, no significant change in hardness was found on the steel side compared with BM S45C (248 ± 9.8 HV). However, the hardness on the Al alloy side (78.5 ± 3.6 HV) was lower than that of BM AA6061-t6 (110 ± 4.2 HV). This softening BM AA6061-t6 could be understood as the dissolution of precipitates caused by the elevated temperature (575 °C) [22]. As shown in Figure 10b, the shear load and IMC

layer thickness were simultaneously enhanced by increasing the holding time. The shear load of Joint-12s (1260 ± 48 N) was higher than that of Joint-0s (1090 ± 42 N) due to the temperature holding time of 12 s. The thickness and type of IMCs are responsible for the mechanical properties of EA-brazing joints of steel and aluminum alloys. An IMC layer that is too thick (greater than 10 μm) tends to cause fatigue crack initiation [13]. In addition, a large amount of embrittlement IMCs, such as $FeAl_2$, $FeAl_3$, and Fe_2Al_5, can significantly reduce the strength of the joint [16]. Therefore, the mechanical properties of the joints of steel and Al alloys can be optimized by adjusting the thickness and type of the IMCs. In this present study, the higher mechanical properties of Joint-12s depend on the relatively thick IMC layer (smaller than 10 μm) and the existence of Fe-rich IMCs (FeAl) compared with Joint-0s [29,30]. The SEM images of the cross-section and corresponding EDS line scanning of the broken Joint-12s are shown in Figure 11. Almost no residual IMCs (Figure 11a,b) were observed on the fracture surface at the S45C steel side; in contrast, the thickness of the remaining IMC layer (Figure 11c,d) on the AA6061-t6 side was measured to be approximately 8.2 μm. Therefore, the bending fracture failure of Joint-12s mainly occurred at the interface between the S45C steel and the IMC layer. This result could be explained by the mechanical interlocking structures formed by the IMCs with needle-like shapes and AA6061-t6.

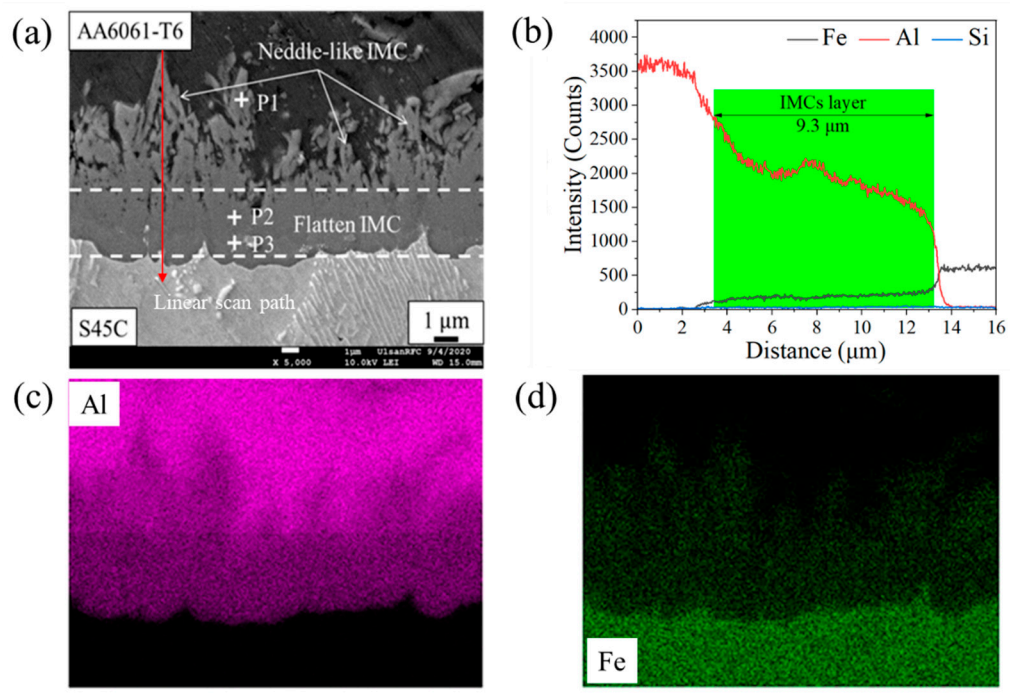

Figure 9. (**a**) SEM micrograph of Joint-12s, (**b**) elemental line scan across the joint interface, (**c**) Al distribution, and (**d**) Fe distribution.

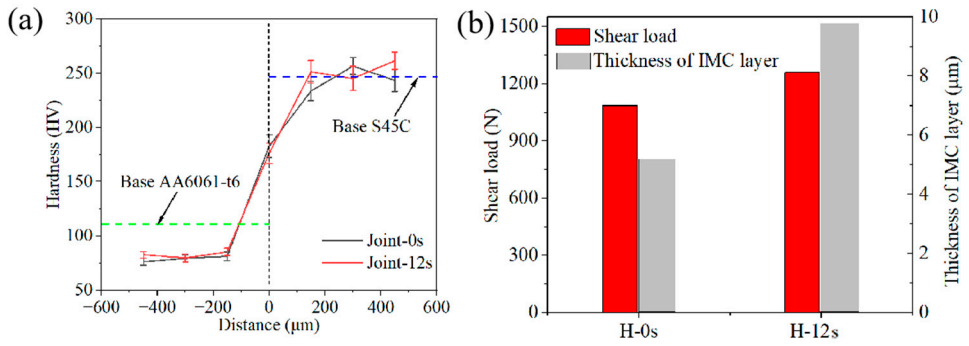

Figure 10. Mechanical properties of EA-brazing joints: (**a**) hardness profiles; (**b**) shear load.

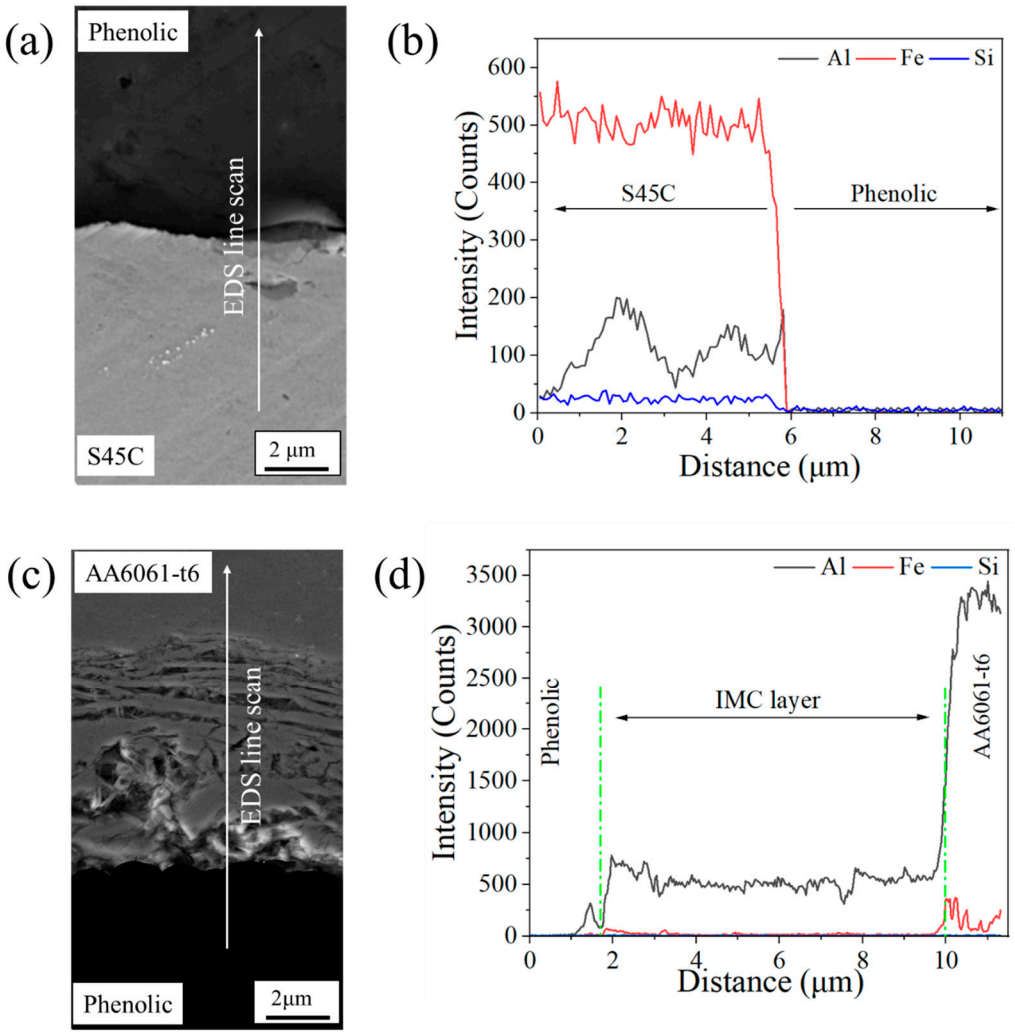

Figure 11. SEM images and elemental line scans of Joint-12s after bending test (**a**,**b**) at the S45C side and (**c**,**d**) at the AA6061-t6 side.

4. Conclusions

In the present work, EA-brazing of S45C steel and 6061-t6 Al alloy was carried out with different temperature holding times. The results of the microstructure analysis indicated that an IMC layer was formed by the mutual diffusion of elements in the Al alloys, steel, and filler in the EA-brazing process. Except for the brittle IMCs ($FeAl_3$ and Fe_2Al_5) present in both joints, the Fe-rich IMCs (FeAl) were observed at the interface of Joint-12s. The thickness of the IMC layer was improved by increasing the temperature-holding time. The comprehensive results of mechanical testing and microstructure analysis suggested that a thicker IMC layer and Fe-rich IMCs appeared to be the leading reason for the improvement in the strength of Joint-12s.

Author Contributions: Conceptualization, K.G.; Software, K.G., G.L. and Y.W.; Data curation, X.S.; Writing—original draft, K.G.; Writing—review & editing, K.G.; Funding acquisition, Y.W. All authors have read and agreed to the published version of the manuscript.

Funding: This work was funded by the Doctoral Research Initiation Fund Program (XB2023006) funded by the Liaoning University of Technology and Youth Project Fund of Liaoning Provincial Department of Education (JYTQN2023223). This work was also supported by Anhui Polytechnic University.

Institutional Review Board Statement: Not applicable.

Informed Consent Statement: Not applicable.

Data Availability Statement: The raw/processed data required to reproduce these findings cannot be shared at this time as the data also form part of an ongoing study.

Conflicts of Interest: The authors declare no conflicts of interest.

References

1. Song, J.L.; Lin, S.B.; Yang, C.L.; Fan, C. Effects of Si additions on intermetallic compound layer of aluminum–steel TIG welding–brazing joint. *J. Alloys Compd.* **2009**, *488*, 31–40. [CrossRef]
2. Nasiri, A.M.; Li, L.; Kim, S.H.; Zhou, Y.; Weckman, D.C.; Nguyen, T.C. Microstructure and Properties of Laser Brazed Magnesium to Coated Steel. *Weld. J.* **2011**, *90*, 212–219.
3. Qiu, R.F.; Iwamoto, C.; Satonaka, S. The influence of reaction layer on the strength of aluminum/steel joint welded by resistance spot welding. *Mater. Charact.* **2009**, *60*, 156–159. [CrossRef]
4. Hokamoto, K.; Nakata, K.; Moria, A.; Tsuda, S.; Tsumura, T.; Inoue, A. Dissimilar material welding of rapidly solidified foil and stainless steel plate using underwater explosive welding technique. *J. Alloys Compd.* **2009**, *472*, 507–511. [CrossRef]
5. Liu, X.; Lan, S.H.; Ni, J. Analysis of process parameters effects on friction stir welding of dissimilar aluminum alloy to advanced high strength steel. *Mater. Design* **2014**, *59*, 50–62. [CrossRef]
6. Ogura, T.; Saito, Y.; Nishida, T.; Nishida, H.; Yoshida, T.; Omichi, N.; Fujimoto, M.; Hirose, A. Partitioning evaluation of mechanical properties and the interfacial microstructure in a friction stir welded aluminum alloy/stainless steel lap joint. *Scr. Mater.* **2012**, *66*, 531–534. [CrossRef]
7. Das, H.; Jana, S.S.; Pal, T.K.; De, A. Numerical and Experimental Investigation on Friction Stir Lap Welding of Aluminum to Steel. *Sci. Technol. Weld. Join.* **2014**, *19*, 69–75. [CrossRef]
8. Acarer, M.; Demir, B. An investigation of mechanical and metallurgical properties of explosive welded aluminum–dual phase steel. *Mater. Lett.* **2008**, *62*, 4158–4160. [CrossRef]
9. Zhang, Y.F.; Huang, J.H.; Cheng, Z.; Zheng, Y.; Chi, H.; Li, P.; Chen, S. Study on MIG-TIG double-sided arc welding-brazing of aluminum and stainless steel. *Mater. Lett.* **2016**, *172*, 146–148. [CrossRef]
10. Lin, S.B.; Song, J.L.; Yang, C.L.; Fan, C.L.; Zhang, D.W. Brazability of dissimilar metals tungsten inert gas butt welding–brazing between aluminum alloy and stainless steel with Al–Cu filler metal. *Mater. Design* **2010**, *31*, 2637–2642. [CrossRef]
11. Findik, F. Recent developments in explosive welding. *Mater. Design* **2011**, *32*, 1081–1093. [CrossRef]
12. Milani, A.M.; Paidar, M.; Khodabandeh, A.; Nategh, S. Influence of filler wire and wire feed speed on metallurgical and mechanical properties of MIG welding-brazing of automotive galvanized steel/5754 aluminum alloy in a lap joint configuration. *Int. J. Adv. Manuf. Tech.* **2016**, *09*, 1495–1506. [CrossRef]
13. Yang, J.; Oliveira, J.P.; Li, Y.; Tan, C.; Gao, C.; Zhao, Y.; Yu, Z. Laser techniques for dissimilar joining of aluminum alloys to steels: A critical review. *J. Mater. Process. Technol.* **2022**, *301*, 117443. [CrossRef]
14. Liu, P.; Li, Y.J.; Wang, J.; Guo, J.S. Investigation of interfacial structure of Mg/Al vacuum diffusion-bonded joint. *Vacuum* **2006**, *80*, 395–399.
15. Yang, J.L.; Xue, S.B.; Xue, P.; Lv, Z.P.; Long, W.; Zhang, G.; Zhang, Q.; He, P. Development of Zn–15Al–xZr filler metals for Brazing 6061 aluminum alloy to stainless steel. *Mater. Sci. Eng. A* **2016**, *651*, 425–434. [CrossRef]
16. Dong, H.; Hu, W.; Duan, Y.; Wang, X.; Dong, C. Dissimilar metal joining of aluminum alloy to galvanized steel with Al–Si, Al–Cu, Al–Si–Cu and Zn–Al filler wires. *J. Mater. Process. Technol.* **2012**, *212*, 458–464. [CrossRef]
17. Qin, G.L.; Ji, Y.; Ma, H.; Ao, Z.Y. Effect of modified flux on MIG arc brazing-fusion welding of aluminum alloy to steel butt joint. *J. Mater. Process. Technol.* **2017**, *245*, 115–121. [CrossRef]
18. Mathieu, A.; Pontevicci, S.; Viala, J.; Cicala, E.; Matteï, S.; Grevey, D. Laser brazing of a steel/aluminium assembly with hot filler wire (88% Al, 12% Si). *Mater. Sci. Eng. A* **2006**, *435–436*, 19–28. [CrossRef]
19. Luu, V.T.; Dinh, T.K.A.; Das, H.; Kim, J.-R.; Hong, S.-T.; Sung, H.-M.; Han, H.N. Diffusion Enhancement during Electrically Assisted Brazing of Ferritic Stainless Steel Alloys. *Int. J. Precis. Eng. Manuf. Technol.* **2018**, *5*, 613–621. [CrossRef]
20. Liu, S.Y.; Suzumura, A.; Ikeshoji, T.; Yamazaki, T. Brazing of Stainless Steel to Various Aluminum Alloys in Air. *JSME Int. J. Series A* **2005**, *48*, 420–425. [CrossRef]
21. Yu, J.; Ge, F.; Yu, G.; Zhang, H.; Fan, Y.; Su, Z.; Gao, J. Feasibility study of thermo-compensated resistance brazing welding of 6061 aluminum alloy to 304 stainless steel. *J. Mater. Res. Technol.* **2023**, *23*, 6200–6215. [CrossRef]
22. Zhang, S.; Gao, K.; Hong, S.T.; Ahn, H.; Choi, Y.; Lee, S.; Han, H.N. Electrically assisted solid state lap joining of dissimilar steel S45C and aluminum 6061-T6 alloy. *J. Mater. Res. Technol.* **2021**, *12*, 271–282. [CrossRef]
23. Gao, K.; Zhang, S.; Mondal, M.; Basak, S.; Hong, S.T.; Shim, H. Friction Stir Spot Butt Welding of Dissimilar S45C Steel and 6061-T6 Aluminum Alloy. *Metals* **2021**, *11*, 1252. [CrossRef]
24. Tanaka, K.; Kumagai, M.; Yoshida, H. Dissimilar joining of aluminum alloy and steel sheets by friction stir spot welding. *J. Jpn. Inst. Light. Met.* **2006**, *56*, 317–322. [CrossRef]
25. Zandsalimi, S.; Heidarzadeh, A.; Saeid, T. Dissimilar friction-stir welding of 430 stainless steel and 6061 aluminum alloy: Microstructure and mechanical properties of the joints. *Proc. Inst. Mech. Eng. Part L J. Mater. Des. Appl.* **2018**, *233*, 1791–1801. [CrossRef]

26. Fereiduni, E.; Movahedi, M.; Kokabi, A.H. Aluminum/steel joints made by an alternative friction stir spot welding process. *J. Mater. Process. Technol.* **2015**, *224*, 1–10. [CrossRef]
27. Bozzi, S.; Helbert-Etter, A.L.; Baudin, T.; Criqui, B.; Kerbiguet, J.G. Intermetallic compounds in Al 6016/IF-steel friction stir spot welds. *Mater. Sci. Eng. A* **2010**, *527*, 4505–4509. [CrossRef]
28. Li, Y.F.; Hong, S.T.; Choi, H.; Han, H. Solid-state dissimilar joining of stainless steel 316L and Inconel 718 alloys by electrically assisted pressure joining. *Mater. Charact.* **2019**, *154*, 161–168. [CrossRef]
29. Arghavani, M.R.; Kokabi, A.H. Role of zinc layer in resistance spot welding of aluminum to steel. *Mater. Design* **2016**, *102*, 106–114. [CrossRef]
30. Pourali, M.; Abdollah-zadeh, A.; Saeid, T.; Kargar, F. Influence of welding parameters on intermetallic compounds formation in dissimilar steel/aluminum friction stir welds. *J. Alloys Compd.* **2017**, *715*, 1–8. [CrossRef]